Aalto Universit

04/17/2024

DEEPlasma GENE Surrogate Model for Tokamak Pedestal Plasma

This work has been carried out within the framework of the EUROfusion Consortium, funded by the European Union via the Euratom Research and Training Programme (Grant Agreement No 101052200 — EUROfusion). Views and opinions expressed are however those of the author(s) only and do not necessarily reflect those of the European Union or the European Commission. Neither the European Union nor the European Commission can be held responsible for them.

Introduction to GENE and microturbulance

Overview

- What is GENE
- Micro Instabilities as Perturbations
- Flux Tube Geometry
- Linear GENE k_y spectrum
- Quasi Linear
- GENE inputs and outputs

What is GENE I

- It is very important to understand **particle and heat transport** to minimise energy losses for fusion **performance**, but also for **fuelling** and **impurity purging**
- The most dominant method for heat and particle transport is **micro-turbulence**
- **Non-linear** GENE can simulate micro-turbulence to compute **heat and particle flux**
- **Linear** GENE can be used to **estimate** the heat and particle flux using a saturation rule, called quasilinear (more later)

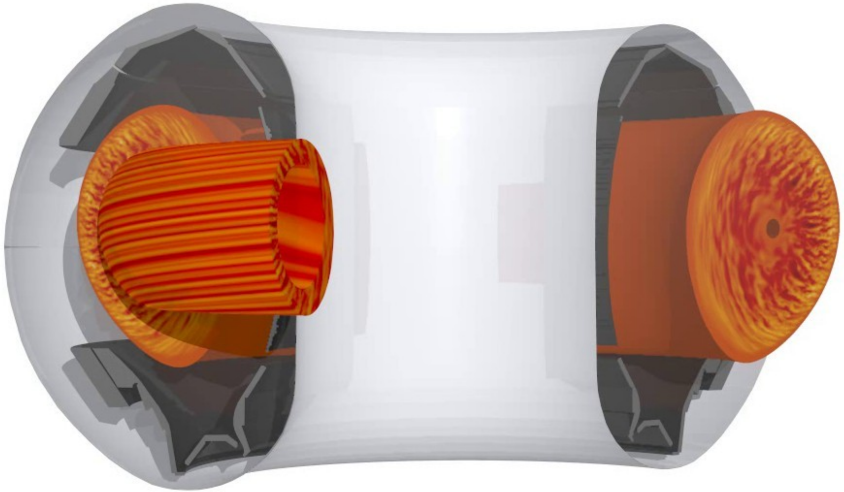

genecode.org

What is GENE II

- Gene is a gyrokinetic code that aims to solve the gyrokinetic Vlasov Maxwell equation; which describes the evolution of the particle distribution.

Terms vanishing due to $\beta = 0$, drop nonlinearity

$$
\begin{aligned}
&\frac{\partial g_j}{\partial t} + \frac{1}{B_{\mathrm{ref}}} \frac{B_0}{B^*_{0\|}} \left(\frac{v_\|^2}{\Omega_j} + \frac{\mu B_0}{m_j \Omega_j} \right) \left[\left(\frac{\partial B_0}{\partial x} - \kappa_2 \frac{\partial B_0}{\partial z} \right) \Gamma_{jy} - \left(\frac{\partial B_0}{\partial y} + \kappa_1 \frac{\partial B_0}{\partial z} \right) \Gamma_{jx} \right] + \frac{B_{\mathrm{ref}}}{J B_0} v_\| \Gamma_{jz} \\
&- \frac{F_{j0}}{B_{\mathrm{ref}}} \frac{B_0}{B^*_{0\|}} \left[L_n^{-1} + \left(\frac{m_j v_\|^2}{2 T_{j0}} + \frac{\mu B_0}{T_{j0}} - \frac{3}{2} \right) L_{Tj}^{-1} \right] \left[c \frac{\partial \chi}{\partial y} + \left(\frac{v_\|^2}{\Omega_j} + \frac{\mu B_0}{m_j \Omega_j} \right) \left(\frac{\partial B_0}{\partial y} + \kappa_1 \frac{\partial B_0}{\partial z} \right) \right] \\
&+ \frac{1}{B_{\mathrm{ref}}} \frac{B_0}{B^*_{0\|}} \frac{4\pi v_\|^2}{B_0 \Omega_j} \frac{\partial p_{j0}}{\partial x} \Gamma_{jy} - \frac{B_{\mathrm{ref}}}{J B_0} \frac{\mu}{m_j} \frac{\partial B_0}{\partial z} \frac{\partial f_j}{\partial v_\|} + \frac{c F_{j0}}{B_{\mathrm{ref}}} \frac{B_0}{B^*_{0\|}} \left(\frac{\partial \chi}{\partial x} \Gamma_{jy} - \frac{\partial \chi}{\partial y} \Gamma_{jx} \right) = \left. \frac{\partial f_j}{\partial t} \right|_{\mathrm{coll}}
\end{aligned}
$$

$$
g_j = f_j - \frac{q_j}{m_j c} \bar{A}_\| \frac{\partial F_{j0}}{\partial v_\|} \quad \chi = \bar{\Phi} - \frac{v_\|}{c} \bar{A}_\| + \frac{\mu}{q_j} \bar{B}_\| \quad \Phi = \frac{\mathcal{C}_3 \mathcal{M}_{00} - \mathcal{C}_2 \mathcal{M}_{01}}{\mathcal{C}_1 \mathcal{C}_3 - \mathcal{C}_2^2} \quad B_\| = \frac{\mathcal{C}_1 \mathcal{M}_{01} - \mathcal{C}_2 \mathcal{M}_{00}}{\mathcal{C}_1 \mathcal{C}_3 - \mathcal{C}_2^2}
$$

$$
\mathcal{M}_{00} = \sum_j \frac{2 q_j}{m_j} \pi B_0 \int J_0 f_j \mathrm{d}v_\| \mathrm{d}\mu \qquad \mathcal{M}_{01} = \sum_j \frac{q_j \pi (2 B_0 / m_j)^{3/2}}{c k_\perp} \int \mu^{1/2} J_1 f_j \mathrm{d}v_\| \mathrm{d}\mu
$$

$$
\mathcal{C}_1 = \frac{k_\perp^2}{4\pi} + \sum_j \frac{q_j^2 n_{j0}}{T_{j0}} (1 - \Gamma_0) \quad \mathcal{C}_2 = -\sum_j \frac{q_j n_{j0}}{B_0} (\Gamma_0 - \Gamma_1) \quad \mathcal{C}_3 = -\frac{1}{4\pi} - \sum_j \frac{m_j n_{j0} v_{Tj}}{B_0^2} (\Gamma_0 - \Gamma_1)
$$

$$
A_\| = \left(\sum_j \frac{8 \pi^2 q_j B_0}{m_j c} \int v_\| J_0 g_j \mathrm{d}v_\| \mathrm{d}\mu \right) \left(k_\perp^2 + \sum_j \frac{8 \pi^2 q_j^2 B_0}{m_j c^2 T_{j0}} \int v_\|^2 J_0^2 F_{j0} \mathrm{d}v_\| \mathrm{d}\mu \right)^{-1}
$$

$$
\Gamma_{jk} = \partial_k g_j + \partial_{v_\|} F_{j0} \partial_k \chi_j q_j / (m_j v_\|) + \bar{A}_\| \partial_k \partial_{v_\|} F_{j0} q_j / (m_j c)
$$

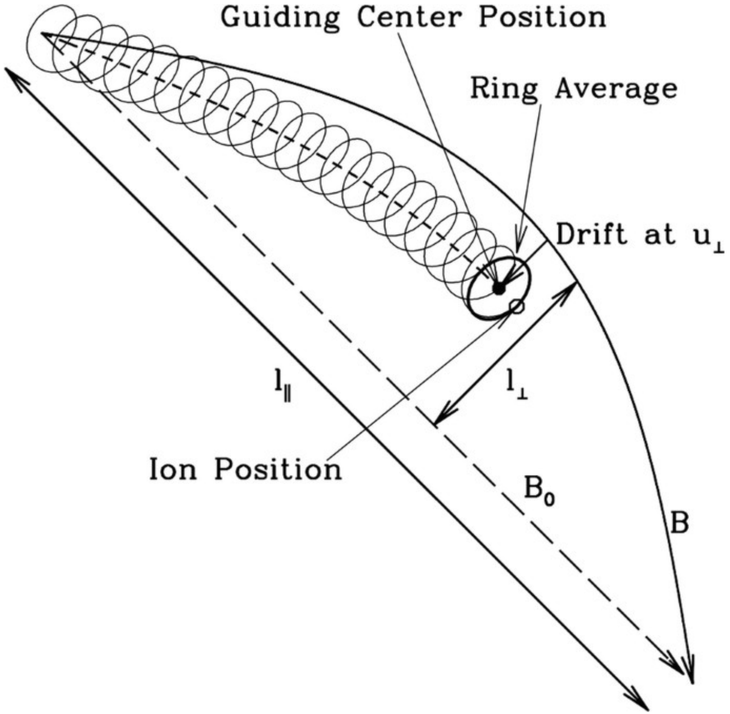

$$
f(\vec{x}, \vec{v}) \rightarrow f(\vec{x}, \mu, v_\|)
$$

Micro Instabilities as Perturbations

$n = n_0 + n_1$

Where n_0 is the equilibrium density for a specific point in space, and n_1 is a small perturbation.

- Looking at the **toy problem** we get an appreciation of what the **growth-rate** of a micro instability is and the difference between **initial value solver and eigenvalue solver**.
- Eigan modes with **-ve** growth rate γ have exponentially **decreasing amplitudes**, these modes are not returned by GENE. **+ve** growth rate modes have exponentially **increasing amplitude** and these are the micro instabilities.
- After some time the **eigenmode** with the **largest gowth rate will dominate**. This is the only growth rate an initial value solver can see. The **eigenvalue solver** can also return **sub-dominant modes.**
- There are an **infinite number of eigenmodes** but the number of **unstable eigenmodes are finite**. The number of eigenmodes in the simulation is dependent on the numerical resolution.
- **Numerical eigenmodes** are not physically present but appear due to 'resonances of the instability with the discretisation of the space'. Great care needs to be taken to ensure there are **no unstable numerical eigenmodes**.

Looking at a simple **toy demo** of the problem. Taylor expansion of some Physics PDE to separate linear and non-linear Terms

$$\frac{\partial n_1}{\partial t} = A n_1 + B {n_1}^2 \ldots$$

An **Initial value solver** numerically computes the RHS of the PDE and multiplies by a small time step Δt to get the density at the next time step. By tracking the change in density over time we can compute the growth-rate of any instability and angular frequency.

$$n_1 = n_{1(t=0)} e^{st}$$

$$s = \gamma + i\omega$$

$$\frac{\partial}{\partial t} n_1 = \Lambda n_1$$

$$n_1 = n_{1(t=0)}\, e^{\gamma t} e^{i\omega t}$$

Alternatively for the Linear part we can use the wave ansatz and solve the **eigenvalue problem**. The perturbation function can be expressed as a linear combination of the eigenfunctions. After some time only the eigenmode with the largest growth rate will dominate.

$$n_1(t) = a\, {n_1}^1 + b\, {n_1}^2 + c\, {n_1}^3 \ldots$$

$${n_1}^1 = e^{\gamma^1 t} e^{i\omega^1 t}$$

Flux Tube Geometry

- The **toy perturbation** on the last slide was looking at a **fixed point in space**. It is often easier to solve PDE’s in **fourier space**.
- GENE can use a **flux tube geometry** or global geometry. Flux tube utilises tokamak symmetry, is less computationally expensive and can completely describe a flux surface.
- The flux tube is **centred on a magnetic field line** that bites its own tail in a one or a few turns around the torus.
- **z** is the along the magnetic field line, **x** is major radially outwards, **y** is perpendicular to both z and x, it is called the diamagnetic direction.
- We often focus on $\mathbf{k_y}$ why it is usually the focus and not k_x or k_z?

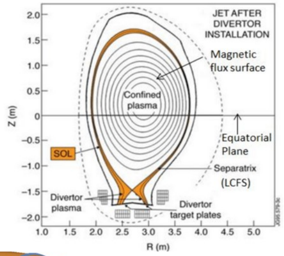

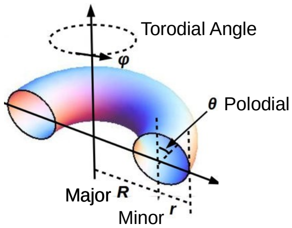

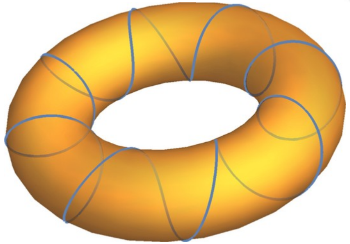

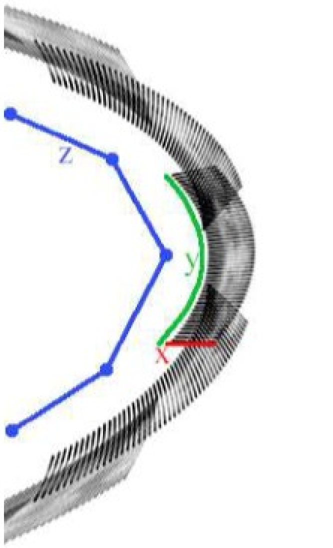

Linear GENE k_y Spectrum

- The plot on the rights shows a **mode transition** between ITG and ETG instabilities that are driven by the ion and electron temperature gradients.
- Does each eigenmode correspond to an instability mode?
- This is the **main output of linear GENE**, growth-rate of micro-instabilities at different ky values.

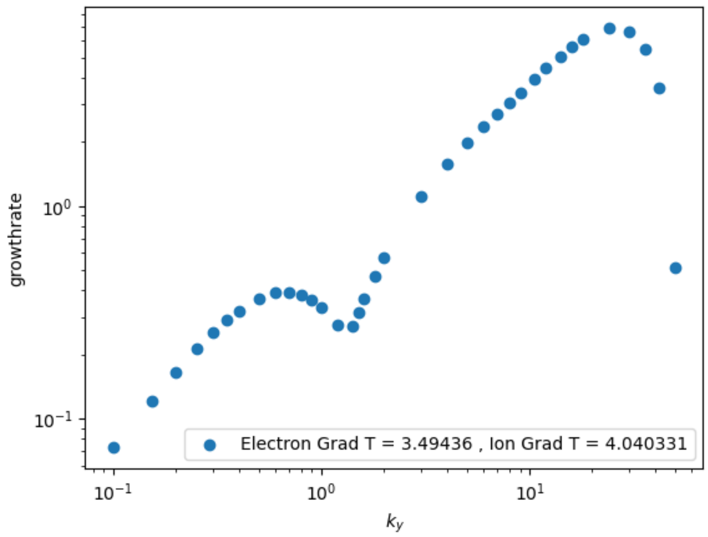

Quasi Linear

- The main difference between linear and non-linear is that **non-linear heat and particle flux saturates**.
- Using **dimensional analysis** we can get a **rough form** for how a growth rate spectrum can be manipulated to compute the **heat flux**.
- A fudge factor (saturation rule), C, needs to be tuned for each k_y so the Quasilinear heat flux matches a non-linear heat flux or an experimental heat flux.

Plasma Phys. Control. Fusion **61** (2019) 034002

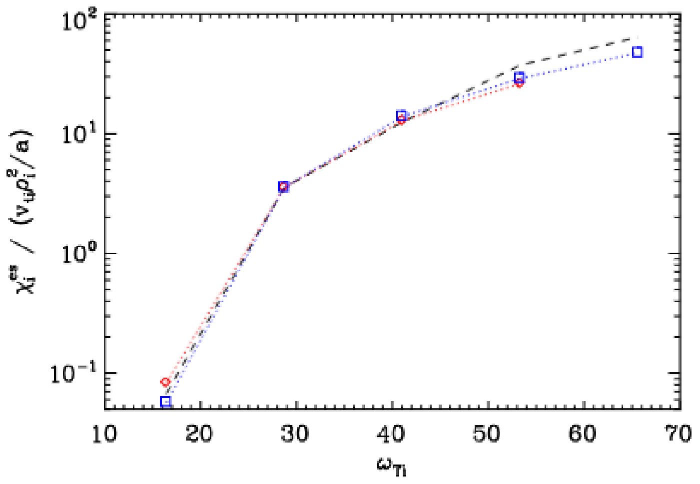

Figure 16. Quasilinear transport modeling. Nonlinear heat diffusivities are shown as a function of driving gradient as a dashed black line. Blue squares denote the quasilinear model using only modes centered at $k_x^{\text{center}} = 0$, whereas the model shown as red diamonds includes finite k_x^{center} modes. Both models are normalized such that they coincide with the nonlinear value at the experimental gradient of $\omega_{Ti} = 28.72$. The quasilinear models perform well, with small deviations appearing at the highest gradients due to proximity to the threshold for strong turbulence.

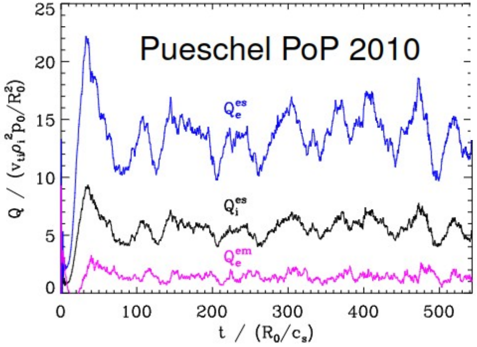

$$Q = -\frac{\nabla T}{T} \sum_{j,k_y} C(k_y) \frac{\gamma(j,k_y)}{< k_\perp(k_y,j)^2 >}$$

GENE Inputs and Outputs

Inputs:
Tokamak major and minor radius

Magnetic Equilibrium
i.e. shape of magnetic flux surfaces

Density and Temperature Profiles
Or Gradients in Flux Tube

Initial particle distribution

Non-Linear Outputs:
Turbulent Heat and Particle flux

Linear Outputs:
Growth rate of each k_y
Angular frequency of each k_y

Lots of Other Outputs:
Some useful for identifying instability modes

Initially the surrogate will focus on one tokamak geometry and magnetic equilibrium, preferably one JET relevant. Then we would train a simple ML model to map from inputs to outputs. Eventually we want to make use of the PDE for physics informed ML.